Developmental Biology 445 (2019) 54–67

Contents lists available at ScienceDirect

Developmental Biology

journal homepage: www.elsevier.com/locate/developmentalbiology

The role of agrin, Lrp4 and MuSK during dendritic arborization and synaptogenesis in cultured embryonic CNS neurons

Gerry Handara[a,b,1], Florian J.A. Hetsch[c,1,2], René Jüttner[c], Anna Schick[a], Corinna Haupt[a], Fritz G. Rathjen[c], Stephan Kröger[a,*]

[a] Department of Physiological Genomics, Biomedical Center, Ludwig-Maximilians-University, Großhaderner Str. 9, D-82152 Planegg-Martinsried, Germany
[b] Institute for Stem Cell Research, German Research Center for Environmental Health, Helmholtz Centre Munich, Ingolstädter Landstraße 1, D-85764 Neuherberg, Germany
[c] Max-Delbrück-Center for Molecular Medicine (MDC), Robert-Rössle-Str. 10, D-13092 Berlin, Germany

ARTICLE INFO

Keywords:
Gephyrin
$GABA_A$ receptor
PSD-95
Autapses
Synaptogenesis
Dendritic arborization

ABSTRACT

The role of agrin, Lrp4 and MuSK, key organizers of neuromuscular synaptogenesis, in the developing CNS is only poorly understood. We investigated the role of these proteins in cultured mouse embryonic cortical neurons from wildtype and from Lrp4- and MuSK-deficient mice. Neurons from Lrp4-deficient mice had fewer but longer primary dendrites and a decreased density of puncta containing excitatory and inhibitory synapse-associated proteins. Neurons from MuSK-deficient mice had an altered dendritic branching pattern but no change in the density of puncta stained by antibodies against synapse-associated proteins. Transfection of TM-agrin compensated the dendritic branching deficits in Lrp4-deficient but not in MuSK-deficient neurons. TM-agrin transfection increased the density of excitatory synaptic puncta in MuSK-deficient but not in Lrp4-deficient mice and reduced the number of inhibitory synaptic puncta irrespective of MuSK and Lrp4 expression. Addition of purified soluble agrin to microisland cultures of cortical neurons revealed an Lrp4-dependent increase in the size and density of glutamatergic synaptic puncta and in mEPSC but not in mIPSC frequency and amplitude. Thus, agrin induced an Lrp4-independent increase in dendritic branch complexity, an Lrp4-dependent increase of excitatory synaptic puncta and an Lrp4- and MuSK-independent decrease in the density of puncta containing inhibitory synapse-associated proteins. These results establish selective roles for agrin, Lrp4 and MuSK during dendritogenesis and synaptogenesis in cultured CNS neurons.

1. Introduction

Synapse formation in the central and peripheral nervous system depends on the coordinated exchange of information between the prospective pre- and postsynaptic cell to generate the pre- and postsynaptic specializations required for successful synaptic transmission (Tintignac et al., 2015; de Wit and Ghosh, 2016). At the neuromuscular junction (NMJ), a key organizer of synaptogenesis is the heparansulfate proteoglycan agrin (Tintignac et al., 2015; Li et al., 2018). According to the agrin hypothesis (McMahan, 1990), agrin is synthesized by motor neurons, secreted by their growth cone while approaching the target muscle fiber, and stably incorporated into the basal lamina of the synaptic cleft. Basal lamina-attached agrin binds to its receptor complex consisting of a tetramer of the agrin-binding low-density lipoprotein receptor-related protein 4 (Lrp4) and the muscle-specific tyrosine kinase MuSK on the skeletal muscle fiber surface (for reviews see Tintignac et al., 2015; Li et al., 2018). The agrin-mediated activation of MuSK and Lrp4 in the muscle fiber plasma membrane subsequently initiates the formation of most, if not all, postsynaptic specializations. In the absence of agrin, Lrp4 or MuSK, motor axons and muscle fibers do not develop synaptic specializations. Instead, motoneuron growth cones continue to extend along the muscle fiber surface, their axons arborize extensively but functional neuromuscular junctions are never established (Gautam et al., 1996, 1999; DeChiara et al., 1996; Weatherbee et al., 2006; Kim et al., 2008; Zhang et al., 2008). Likewise, postsynaptic specializations, including nerve-associated aggregates containing the nicotinic acetylcholine receptor and other molecules involved in synaptic transmission, never develop. Accordingly, these mutant mice are immobile and die perinatally due to respiratory muscle failure.

* Corresponding author.
E-mail address: skroeger@lmu.de (S. Kröger).
[1] Both authors contributed equally to this work.
[2] Current address: Department of Cell Physiology, TU Braunschweig, Spielmannstr. 8, D-38106 Braunschweig, Germany.

https://doi.org/10.1016/j.ydbio.2018.10.017
Received 31 August 2018; Received in revised form 22 October 2018; Accepted 22 October 2018
Available online 29 October 2018
0012-1606/

Compared to the NMJ, the roles of agrin, Lrp4 and MuSK in the developing CNS are much less understood. All three components are expressed in the CNS by neurons and glial cells (Garcia-Osta et al., 2006; Tian et al., 2006; Ksiazek et al., 2007; Sun et al., 2016; Karakatsani et al., 2017; Ye et al., 2018). However, agrin at the neuromuscular junction is synthesized as a secreted, laminin-binding and basal lamina-associated form (NtA-agrin), whereas the majority of agrin in the CNS is the transmembrane form (TM-agrin). In this isoform, alternative first exon usage leads to the replacement of the N-terminal laminin-binding domain by a single transmembrane region and a 28 amino acid (mouse) intracellular domain (Burgess et al., 2000; Neumann et al., 2001).

The widespread expression of agrin by neurons and glial cells has led to the hypothesis that agrin might have a role during interneuronal synaptogenesis, similar to its role at the neuromuscular junction (Kröger and Pfister, 2009; Daniels, 2012). Consistently, expression levels of agrin are high during the period of synapse formation but become downregulated thereafter (Burgess et al., 2000). Agrin is concentrated at interneuronal synapses (Koulen et al., 1999; Ksiazek et al., 2007) and its levels remain high in brain regions with a high degree of synaptic plasticity (Burk et al., 2012). Moreover, agrin expression is upregulated again under conditions that require formation of new synapses or their plastic changes, including seizures or traumatic brain injury (O'Connor et al., 1995; Falo et al., 2008). Conflicting results exist regarding a role for agrin during CNS synaptogenesis. Agrin-deficient mouse embryos display no overt abnormalities in the morphology of CNS synapses (Gautam et al., 1996) and synapse formation of CNS neurons in culture occurred in the absence of agrin (Serpinskaya et al., 1999; Li et al., 1999). On the other hand, adult mice in which the perinatal lethality due to agrin-deficiency was rescued by re-expression of agrin cDNA exclusively in motoneurons, revealed an approximately 30% reduction in dendrite length, spine density and mEPSC frequency in the adult cortex suggesting a role for agrin in the maintenance of excitatory synapses in the CNS (Ksiazek et al., 2007). Potential functional interactions of agrin with Lrp4 or MuSK in shaping the dendritic branching pattern and the formation of excitatory and inhibitory synapses in embryonic CNS neurons were never analyzed.

In this study, we investigated the effect of overexpressing TM-agrin cDNA or application of soluble agrin to embryonic neurons from wildtype, Lrp4^{mitt} mice (representing Lrp4-deficient neurons) and MuSK-deficient mice. We used cortical neurons cultured as monolayers or as isolated single neurons in microisland cultures to test whether agrin affects dendritic morphology or the density of synaptic puncta. We show that embryonic cortical neurons from Lrp4- or MuSK-deficient mice revealed a reduced dendritic branching complexity. The reduced dendritic complexity was compensated by transfection with TM-agrin cDNA in Lrp4-deficient neurons but not in MuSK-deficient neurons. A reduced number of aggregates containing PSD-95 and the NMDA receptor NR-1 subunit was observed in Lrp4-deficient but not in MuSK-deficient neurons. Transfection of TM-agrin in control neurons or in MuSK-deficient neurons increased the number of PSD-95 and NR1 subunit puncta. In contrast, transfection of TM-agrin into Lrp4-deficient neurons did not result in an increase in the density of excitatory synaptic puncta. Lrp4- but not MuSK-deficient neurons had a reduced density of puncta containing gephyrin and of the α1-subunit of the $GABA_A$ receptor. Transfection of TM-agrin into control neurons reduced the density of puncta containing inhibitory synapse-associated proteins independent of Lrp4- or MuSK expression. Incubation of cortical neurons in microisland cultures with soluble agrin increased the amplitude and frequency of mEPSCs but not of mIPSCs. Soluble agrin also promoted the formation of excitatory but not of inhibitory postsynaptic specializations in an Lrp4-dependent manner. Collectively, these results demonstrate differential effects of agrin, Lrp4 and MuSK on dendritic branching complexity and on excitatory and inhibitory synapses. Overall, our data point to functional links between these three proteins in modulating dendritic branching and formation of synaptic specializations in developing CNS neurons.

2. Materials and methods

2.1. Mice

Use and care of animals was approved by German authorities and according to national law (TierSchG§7). C57BL/6N wild-type as well as MuSK-/- (DeChiara et al., 1996) and Lrp4^{mitt} mice (Weatherbee et al., 2006) were bred in the animal facility of the Max-Delbrueck Center Berlin. C57BL/6N mice were bred in the animal facility of the Biomedical Center of the Ludwig-Maximilians-University Munich. Animals were housed on a 12/12 h light/dark cycle with free access to food and water. The animal procedures were performed according to the guidelines from directive 2010/63/EU of the European Parliament on the protection of animals used for scientific purposes. Genotyping of the different mouse strains was performed by PCR analysis. PCR products of Lrp4 genotyping were further subjected to enzymatic digestion with HpyCH4V at 37 °C overnight. PCR products from Lrp4^{mitt} mice gave rise to a single uncleaved band with a length of 227 bp. Wildtype PCR products were completely cleaved and produced two bands of 132 and 69 bp length. In addition, Lrp4-deficient embryos were identified by the syndactyly of their hind- and forelimbs as described by Weatherbee et al. (2006) and by Western blotting with antibodies against Lrp4 (sup. Fig. S8). All experiments were approved by the local authorities of Berlin (LaGeSO; numbers T0313/97 and X9014/15) and Munich (Az.: 55.2-1-54-2532.8-160-13 and 55.1-8791-14.587). The day of the vaginal plug was considered embryonic day 0.5 (E 0.5). Male and female wildtype C57BL/6N mice, MuSK or Lrp4^{mitt} heterozygous littermates, respectively, were used as controls. We did not observe any difference between heterozygous MuSK or Lrp4^{mitt} mice and wildtype animals (see below).

2.2. Microisland cultures

Methods for microisland cultivation of neurons were adapted from Rost et al. (2010). Coverslips 30 mm in diameter were coated with a thin layer of 0.15% low-melting agarose. A custom-made stamp with small dots was then used to create islands by printing with a solution containing 0.85 mg/ml collagen I from rat tail (Thermo Fisher Scientific, Darmstadt, Germany) and 0.1 mg/ml poly-D-lysine (Sigma-Aldrich) on the agarose-coated coverslip. Coverslips were left to dry for 48 h and sterilized under a sterile hood by UV-irradiation for at least 30 min.

Astrocytes were obtained from cortices of P0 up to P2 wildtype C57BL/6N or E18.5 mutant mice and cultivated according to standard procedures (McCarthy and de Vellis, 1980) in DMEM supplemented with 10% FCS and P/S for at least 14 days before seeding them on microislands at a concentration of 50.000 cells/ml and cultivated for at least 4 days on the pre-coated coverslips. Lrp4-deficient neurons were grown on Lrp4-deficient astrocytes that were prepared from cortices of E18.5 embryos. Neurons were seeded at a concentration of 3.000 cells per ml on microislands with pre-grown astrocytes. Neurons were cultivated for 5–6, 10–11 or 12–15 days *in vitro* (DIV) in neurobasal medium (Invitrogen) supplemented with B27 supplement (Thermo Fisher Scientific), BME amino acid solution (Sigma Aldrich, Munich, Germany) and GlutaMAX (Thermo Fisher Scientific). Cultures were treated with 1 µg/ml soluble chick agrin 3–5 h before they were subjected to electrophysiological analyses or immunocytochemistry. In initial experiments soluble chick agrin748 at concentrations ranging from 50 ng/ml to 5 µg/ml was applied for 3–5 h to monolayer cultures followed by electrophysiological recordings. A concentration of 1 µg/ml of soluble agrin was sufficient to increase the mEPSC frequency response to maximal levels.

2.3. Monolayer cultures

Primary monolayer cultures from E15 cortices of heterozygous or homozygous MuSK-deficient, or Lrp4^{mitt} mouse embryos were prepared by trypsinization and trituration with fire-polished Pasteur pipettes as described (Brewer et al., 1993; Karakatsani et al., 2017). To this end, 18 mm coverslips were pre-treated overnight with NaOH/EtOH, 1 M HCl and stored in absolute ethanol. Coverslips were then coated with poly-D-lysine overnight under sterile conditions in an incubator and then washed with sterile water. Embryonic neurons were seeded at a density of 100.000 cells per well (12-well plate, growth area 3.8 cm^2/well) and cultivated for 8 or 14 days *in vitro* (DIV) in neurobasal medium (Invitrogen) supplemented with B27 supplement (Thermo Fisher Scientific), GlutaMAX (Thermo Fisher Scientific) and penicillin-streptomycin.

We did not detect any differences in the density of viable cells (DAPI-positive), of neurons in general (NeuN-positive cells) and of inhibitory neurons (GABA-positive) between cultured neurons from wildtype- or heterozygous littermates or from MuSK-deficient- or homozygous Lrp4^{mitt} mice (sup. Fig. S7), demonstrating that cortical neuronal cultures from Lrp4- and MuSK-deficient mice were similar with respect to the cellular density and neuronal composition compared to cultures from their respective heterozygous littermates. Consistently, the brain of mice overexpression agrin using a bacterial artificial chromosome containing the entire *Agrn* gene, as well as 7 kb of upstream DNA and 30 kb of downstream DNA displayed no overt neurological phenotypes such as tremor, seizures, or ataxia and no histological changes in several brain areas (Fuerst et al., 2007). There was also no difference in any aspect analyzed in our study between neurons from wildtype and neurons from the respective heterozygous mice. Therefore, neurons from heterozygous mice (Lrp4^{mitt}+/- and MuSK+/- mice) were used as controls throughout this study.

2.4. Antibodies and immunocytochemistry

Neuronal cultures were fixed either in methanol solution for 10 min at − 20 °C or in 4% paraformaldehyde in PBS for 10 min at room temperature (depending on the optimal preservation of the antigenicity) followed by washing, blocking and permeabilization with 2% bovine serum albumin and 0.2% Triton X-100 in PBS (Zhang et al., 2015; Karakatsani et al., 2017). The following antibodies were applied: anti-PSD95 (mouse monoclonal IgG2a, clone 7E3-1B8, Cat. No. MA1-046, Thermo Fisher Scientific; mouse monoclonal, clone K28/43, Cat. No. Mab68, Merck, Darmstadt, Germany); anti-VGluT1 (polyclonal guinea pig antiserum, Cat. No. 135304, Synaptic Systems, Göttingen, Germany); anti-VGluT2 (polyclonal guinea pig antiserum, Cat. No. 135404, Synaptic Systems); anti-gephyrin (rabbit polyclonal antiserum, Cat. No. 147002, Synaptic Systems; mouse monoclonal, clone mAb7a, Cat. No. 147021, Synaptic Systems); anti-GABA$_A$ receptor α1-subunit (rabbit polyclonal, Cat. No. 06–868, Merck, Darmstadt, Germany); anti-NMDA receptor NR1-subunit (mouse monoclonal, Cat. No. Mab363, Merck), anti-GluA, AMPA receptor (monoclonal mouse purified IgG, clone 248B7, Cat. No. 182411, Synaptic Systems), anti-NeuN (mouse monoclonal, Cat. No. mab377, Merck), anti-GABA (rabbit polyclonal, Cat. No. A2052, Merck); anti-GFP (chicken polyclonal, Cat. No. ab13970, Abcam); anti-agrin (rabbit polyclonal against the C-terminal 95 kDa fragment (Eusebio et al., 2003), detects all isoforms of agrin and reacts with TM-agrin as well as with NtA-agrin); anti-Lrp4 antibody (rabbit polyclonal, H-98, Cat. No. sc-98775; Santa Cruz Biotechnology). As secondary antibodies, we used highly pre-absorbed, Alexa Fluor-conjugated antibodies directed against the appropriate species and monoclonal isotype (Alexa 488, 594 and 647, Thermo Fisher Scientific). A detailed list of the antibodies is available online as key resource table.

2.5. Electrophysiology

Coverslips were submerged in pre-warmed extracellular solution containing 105 mM NaCl, 3 mM KCl, 10 mM HEPES, 5 mM Glucose, 2 mM $CaCl_2$, 1 mM $MgCl_2$. Cells were visually inspected using a 40× water immersion objective and an upright Zeiss Axioscope 2 FS equipped with phase contrast optics. Special care was taken to ensure that only one neuron was present on a given island. Pipettes pulled from borosilicate glass (Item # 1B150F-4; World Precision Instruments, Sarasota, USA) using a model P-97 micropipette puller (Sutter Instrument, Novato, USA) were filled with intracellular solution containing 90 mM KCl, 3 mM NaCl, 5 mM EGTA, 5 mM HEPES, 5 mM Glucose, 0.5 mM $CaCl_2$, 4 mM $MgCl_2$. Pipettes had resistances of around 3–5 MΩ when filled with intracellular solutions. Cells were analyzed in whole cell voltage clamp mode. The passive membrane properties are comprised of the cell's capacitance (Cm) and its membrane resistance (R_{in}). The access resistance (R_a) was determined by measuring the maximal transient current (Imax) which is induced if a cell's membrane potential is depolarized by + 10 mV (ΔU) using the formula $R_a = \Delta U/Imax$. Cells exceeding an uncompensated access resistance of 30 MΩ were discarded. The input resistance of a cell was computed by measuring the offset current (I_{Offset}) of the current response and dividing ΔU by it. To determine the membrane capacitance of a cell a 200 ms voltage change was induced in its membrane potential by + 10 mV for 10 times. The acquired trace was averaged and the integral of the current response, the charge of the membrane, was determined, giving rise to the membrane capacitance as can be deduced by these formulae:

$$Cm = 1/\Delta U * \int Idt = Charge/\Delta U = pF;\ Charge = pA * s = pC.$$

Miniature postsynaptic currents (mPSCs) were recorded in the presence of 1 μM TTX. Application of additional drugs was not necessary since inhibitory and excitatory postsynaptic currents of single neurons could be distinguished by their decay time kinetics (τ for mEPSCs 1–6 ms, τ for mIPSCs > 10 ms). mPSCs were always recorded at a holding potential of − 70 mV in voltage clamp mode by using a 10 s recording protocol which was repeated 10 times. The reversal potentials E_{rev} for Cl^- and for Na^+ were calculated to be -2.81 and 89.81 mV, respectively. Under these conditions, GABA- and glutamate-induced currents both have an inward direction.

The quantal size was determined by histograms of the mPSC amplitude distribution of a neuron using Origin7.0 (OriginLab, Northampton, USA). The peak of the histogram was measured to determine the quantal size of the mPSCs in a given cell. A bin size of 2 pA was selected and only cells with > 100 events were analyzed. This gives an estimate of the current that is evoked by a single vesicle release. To determine the quantal content of evoked postsynaptic events the values of the mean amplitudes of the first synaptic responses were divided by the mean values of the quantal size of either excitatory or inhibitory miniature postsynaptic currents giving a rough estimate of how many vesicles were released. Therefore, the quantal content represents an average of different synapses from an individual neuron. However, only synapses of the same type (GABAergig or glutamatergic) were grouped. This calculation was required since recordings of autaptic currents and recordings of mPSCs from the same neuron did not result in a sufficient number of miniature events to calculate the quantal size.

Neurotransmitter release in microisland cultures was studied in single neurons making autaptic connections without the need for extracellular stimulation. Autaptic connections (aEPSCs and aIPSCs) were revealed by a brief (1 ms) step of the membrane potential to 0 mV. The paired pulse ratios were determined for inter stimulus intervals (ISI) of 100 ms. For high-frequency stimulation experiments neurons were stimulated at 10 Hz (ISI = 100 ms) for inhibitory cells or at 50 Hz (ISI = 20 ms) for excitatory cells, repeating the stimulus regime

10 times with a pause of 5 s between stimuli and averaging the responses. Recordings were performed at ambient temperature (20–22 °C).

All electrophysiological data were analyzed offline using TIDA 5.24 (HEKA Elektronik GmbH, Lambrecht, Germany). Miniature postsynaptic currents (mPSCs) were analyzed using Peak-Count programmed by Christian Henneberger (version 2.02; Henneberger et al., 2002).

2.6. Transfection

Transfection of cortical neurons with Lipofectamine 2000 (Invitrogen) was performed on DIV 12 as previously described (Karakatsani et al., 2017). The number of transfected cells was in the range of 2% and the efficiency was similar independent of the vector used. Agrin was overexpressed using a full-length TM-agrin cDNA from mouse cloned into the bicistronic pMES vector (Swartz et al., 2001; Schröder et al., 2007; Karakatsani et al., 2017). This vector contains an internal ribosomal entry site regulating the simultaneous expression of the gene of interest together with the enhanced green fluorescent protein. This allowed the convenient distinction of the few transfected from the untransfected cells. Full-length mouse TM-agrin cDNAs coding for the neuronal TM-agrin isoform (y4z8) was cloned into the multiple cloning site of the pMES vector. Transfection of a pMES vector without an agrin cDNA insert was used as control. All constructs used in this study were routinely sequenced and subject to diagnostic restriction digest to eliminate the possibility of mutations.

2.7. Quantitative analysis of dendritic morphology and synaptic puncta

The numbers of primary dendrites emerging from the soma as well as the dendritic branch tip numbers were counted manually. Axons were excluded from the analysis. The dendritic length in µm was determined using the Fiji Simple Neurite Tracer plugin (Longair et al., 2011) in cortical neurons using the images obtained with an Axio ImagerM2 epifluorescence microscope (Carl Zeiss). For analyses of the dendritic branching pattern, images were converted into 8-bit format and Sholl analysis was performed on the thresholded form of these binary images using the Fiji plugin (Ferreira et al., 2014).

For puncta density analyses of synapse-associated proteins, images were converted into 8-bit format and a binary image was created using an appropriate threshold. Axons were excluded from the analysis. Three dendrites per neuron were randomly selected and subjected for further analysis. The density of puncta of synapse-associated proteins was counted using the Analyze Particle toolbox of the Fiji software. Since excitatory and inhibitory synapses are not evenly distributed along the dendrite, the number of puncta per 20 µm associated with excitatory synapses was determined on distal dendrites outside a 50 µm radius from the soma (Klenowski et al., 2015). In contrast, punctate immunoreactivity with antibodies against inhibitory synapses was determined on dendrites within a radius of 50 µm from the soma (Klenowski et al., 2015).

2.8. Quantitative analysis of synaptic puncta in microisland cultures

Images of single neurons for quantification of synaptic puncta (VGlut1+2 and PSD95) and for AMPAR cluster area (VGlut1+2 and GluA) were acquired using a LSM700 confocal microscope (Carl Zeiss GmbH, Jena) equipped with a 63× oil objective and ZEN 2010 software. The soma of a neuron was placed in the center of the image and a zoom factor of 0.5 was chosen. For AMPA receptor cluster area evaluation a zoom factor of 1.5 was chosen. Z-Stack images were acquired at the suggested z-intervals by the software and transformed into 2D images using maximal intensity projections for analysis.

Synaptic puncta were counted using the PunctaAnalyzer plugin for ImageJ (written by Barry Wark; Ippolito and Eroglu, 2010). In brief, a region of interest comprising the whole field of view (203.23 µm by 203.23 µm) of the image was drawn. Puncta were thresholded for each individual channels, a minimum puncta size of four pixels was chosen and colocalized puncta were counted by the software.

AMPA receptor cluster area and density in microisland cultures were analyzed using ImageJ. AMPA receptor fluorescence was thresholded and the area of colocalization with VGlut1+2 was determined by drawing a region of interest around colocalized spots and measuring the area of that specific area. Density of AMPA receptors on dendrites was determined manually by measuring the dendrite length and counting AMPA receptor-positive puncta on the respective dendrites.

2.9. Statistical analysis

Results are presented as mean + SEM. Values for N represent the number of independent experiments, *i.e.* the number of animals. Values for n represent the number of cultures/cells analyzed. With the assumption of normal distribution and homoscedasticity, significance was calculated with GraphPad Prism vs.7 (GraphPad Software, San Diego, California) using the unpaired *t*-test or the one-way ANOVA test with the Tukey's multiple comparison test. Statistical analysis of electrophysiological data was performed using SigmaStat (vs. 3.5; Systat Software GmbH, Erkrat, Germany). Data were evaluated for normal distribution and for homoscedasticity using the D'Agostino & Pearson normality test or Browne-Forsythe's test. Data that did not fulfil the assumption were investigated using the equivalent non-parametric tests, such as the Mann-Whitney rank sum test or the Kruskal-Wallis-test with Dunn's correction for multiple comparisons test. Outliers were determined by Grubbs' test with iteration and were excluded for the statistical analysis. The type 1 statistical error was set to 5% ($\alpha = 0.05$). A p level of < 0.05 was set as the level of statistical significance.

3. Results

3.1. Lrp4-independent changes in dendritic branching pattern induced by TM-agrin transfection

The aim of this study was to analyze the role of Lrp4, MuSK and agrin in developing CNS neurons. As a first step, we analyzed the dendritic morphology of embryonic cortical neurons from homozygous embryonic Lrp4^{mitt} mice. These mice lack Lrp4 and die perinatally due to failure in neuromuscular junction formation (Weatherbee et al., 2006). The dendritic branching pattern of embryonic cortical neurons from homozygous Lrp4^{mitt} mice cultured for 12 days was significantly altered compared to neurons in parallel cultures from heterozygous Lrp4^{mitt} control mice (Fig. 1A,B). Quantification demonstrated a reduction of the number of primary dendrites (Fig. 1D) and of the density of dendritic spines (Fig. 1E). Moreover, Sholl analysis revealed a reduced number of intersections particularly at a radius between 20 and 80 µm from the cell body (Fig. 1F). A similar reduction of the dendritic arborization complexity was detected by analyzing the Schoenen Ramification Index (sup. Fig. S1A) as well as the maximal number of branching (sup. Fig. S1B) and the total dendritic branch tip number (sup. Fig. S1C), confirming that Lrp4 is required for the establishment of the normal dendritic branching pattern.

To analyze the role of agrin during establishment of the dendritic branching pattern, we transfected cultured cortical neurons with a cDNA coding for GFP (control vector) or with a vector coding for GFP plus full-length mouse TM-agrin (isoform y4z8; Fig. 1C). Transfection of neurons from heterozygous Lrp4^{mitt} mice increased the number of spines (Fig. 1E), but did not alter the number of primary dendrites or the branching pattern of the transfected neurons (Fig. 1D, F). In contrast, transfection of TM-agrin cDNA into neurons from homozygous Lrp4^{mitt} mice reversed the changes in the dendritic morphology observed in Lrp4-deficient neurons, including the number of primary

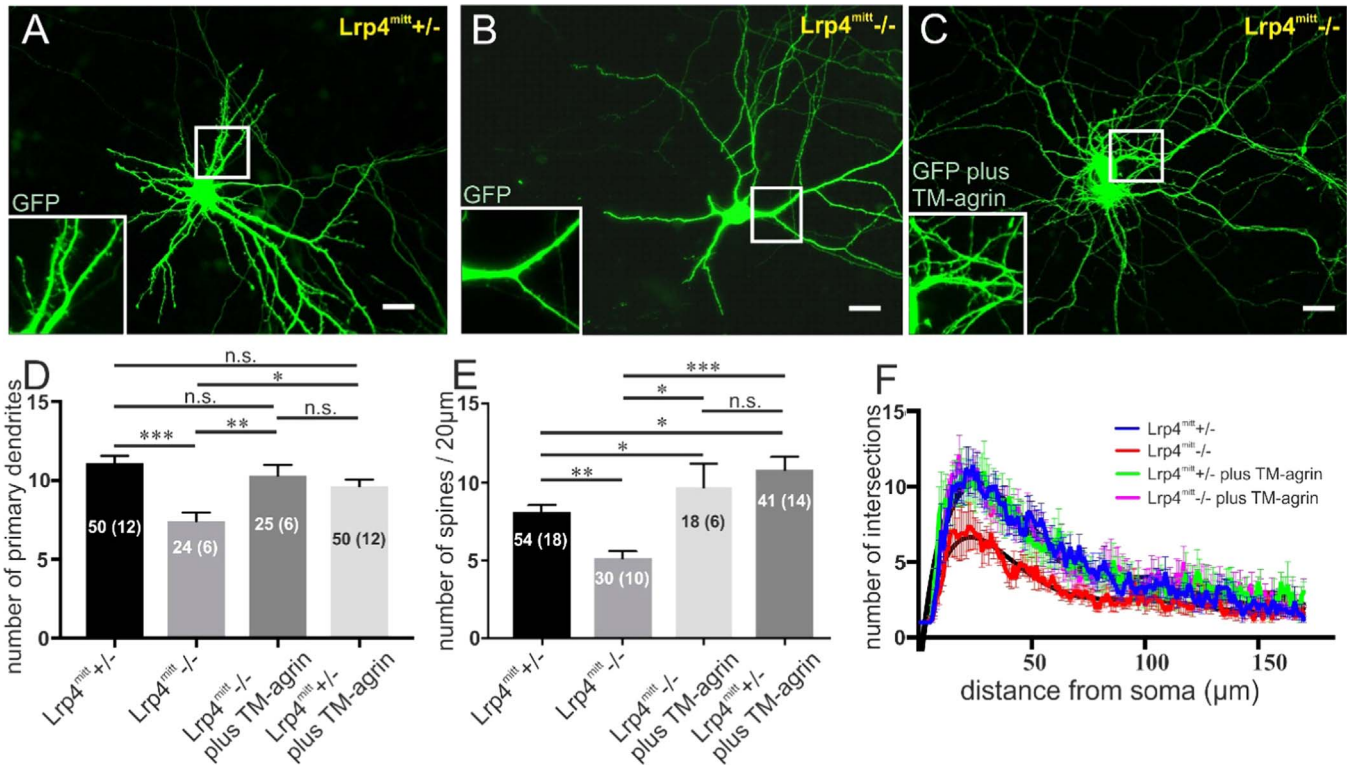

Fig. 1. Cultured neurons from Lrp4^{mitt} mice exhibit an altered dendritic morphology and transfection with TM-agrin restores normal dendritic arborization pattern. The morphology of heterozygous (panel A) and homozygous (panel B) Lrp4^{mitt} neurons is shown after DIV 14. Cells were transfected at DIV 12 with either a control vector coding for GFP (A, B) or with a vector coding for GPF plus full-length mouse TM-agrin (C). The insets in panels A–C show higher magnifications of the boxed area to reveal the density of neurites/spines. Quantification revealed a significantly reduced number of primary dendrites (panel D) and of the density of dendritic spines (panel E) in homozygous Lrp4-deficient neurons, compared to neurons from heterozygous littermates. Likewise, Sholl analysis revealed a reduced number of intersections in neurons from homozygous Lrp4^{mitt} mice compared to heterozygous littermates (panel F). Transfection with TM-agrin increased all three parameters to control values in neurons from heterozygous and homozygous Lrp4^{mitt} mice. The mean + SEM is shown in panels D and E. Numbers in columns represent the number of neurons (n) and, in parentheses, the number of animals (N) analyzed. Kruskal-Wallis-Test with Dunn's correction for multiple comparison was applied. The unpaired *t*-test was applied specifically for comparing the spine density between neurons from heterozygous and homozygous Lrp4^{mitt} mice (E). The fitting curves (black) in panel F were generated using Graphpad Prism. Scale bar in A–C: 10 µm.

dendrites (Fig. 1D), number of spines (Fig. 1E), number of intersections in Sholl analysis (Fig. 1F), Schoenen Ramification Index (sup. Fig. S1A), maximal number of branching (sup. Fig. S1B) and the total dendritic branch tip number (sup. Fig. S1C). These results show that TM-agrin overexpression can ameliorate the changes in the dendritic branching pattern caused by lack of Lrp4 expression.

We observed an increase in the density of filopodia-like protrusions extending from the dendrite in TM-agrin transfected neurons, similar to what has been reported previously (see insets in Fig. 1C; McCroskery et al., 2009; Ramseger et al., 2009; Porten et al., 2010). The formation of these processes was also independent of Lrp4 expression.

Interestingly, the primary dendrite of neurons from homozygous Lrp4^{mitt} mice was longer compared to neurons from heterozygous Lrp4^{mitt} mice (sup. Fig. S1D). Thus, neurons from Lrp4^{mitt} mice had a similar phenotype as wildtype neurons treated with miLrp4 RNA (Karakatsani et al., 2017). The transfection with the full-length TM-agrin cDNA reduced the length of the primary dendrite in neurons irrespective of Lrp4 expression, demonstrating that agrin's effect in dendritic branching pattern was independent of Lrp4 (sup. Fig. S1D). Collectively, our results provide evidence for independent roles of Lrp4 and agrin in shaping the dendritic morphology of embryonic CNS neurons.

3.2. The TM-agrin-mediated increase in excitatory synapse-associated protein puncta depends on the expression of Lrp4

To investigate if the density of excitatory synapses was altered in neurons from Lrp4^{mitt} mice we analyzed the number of puncta on dendrites stained with antibodies against PSD-95 and against the NR1-subunit of the NMDA receptor. We observed that the density of dendritic PSD-95 puncta in neurons from homozygous Lrp4^{mitt} mice was significantly reduced compared to neurons from heterozygous littermate controls (Fig. 2A, C). Quantification revealed that neurons from homozygous Lrp4^{mitt} mice had approximately 50% of the density of PSD-95 puncta (Fig. 2E) and 35% of the density of NR1 subunit puncta (Fig. 2F) on their dendrites compared to neurons from heterozygous control mice. These results show that Lrp4 expression is required for the formation and/or maintenance of glutamatergic synapse-like specializations on dendrites of embryonic CNS neurons.

Next, we investigated if the decreased density of PSD-95 puncta in neurons from Lrp4^{mitt} mice was influenced by transfection with a cDNA coding for full-length mouse agrin (isoform y4z8). Overexpression of TM-agrin in cortical neurons from heterozygous Lrp4^{mitt} control mice significantly increased the number of dendritic PSD-95 and NR1 subunit puncta (Fig. 2B, E, F and sup. Fig. S2). In contrast, overexpression of the same cDNA construct in Lrp4-deficient neurons did not affect the density of PSD-95 and NR1 puncta compared to neurons of the same genotype transfected with the control vector (Fig. 2D–F and sup. Fig. S2). These results show that the increase in the density of excitatory synapse-associated protein puncta after transfection of TM-agrin depended on the expression of Lrp4.

3.3. Loss of Lrp4 results in a TM-agrin-independent decrease in the density of inhibitory synapse-associated protein puncta

To investigate if Lrp4 expression also affected the formation of inhibitory synaptic specializations and to determine if TM-agrin over-expression had a similar effect on the density of inhibitory synapse-

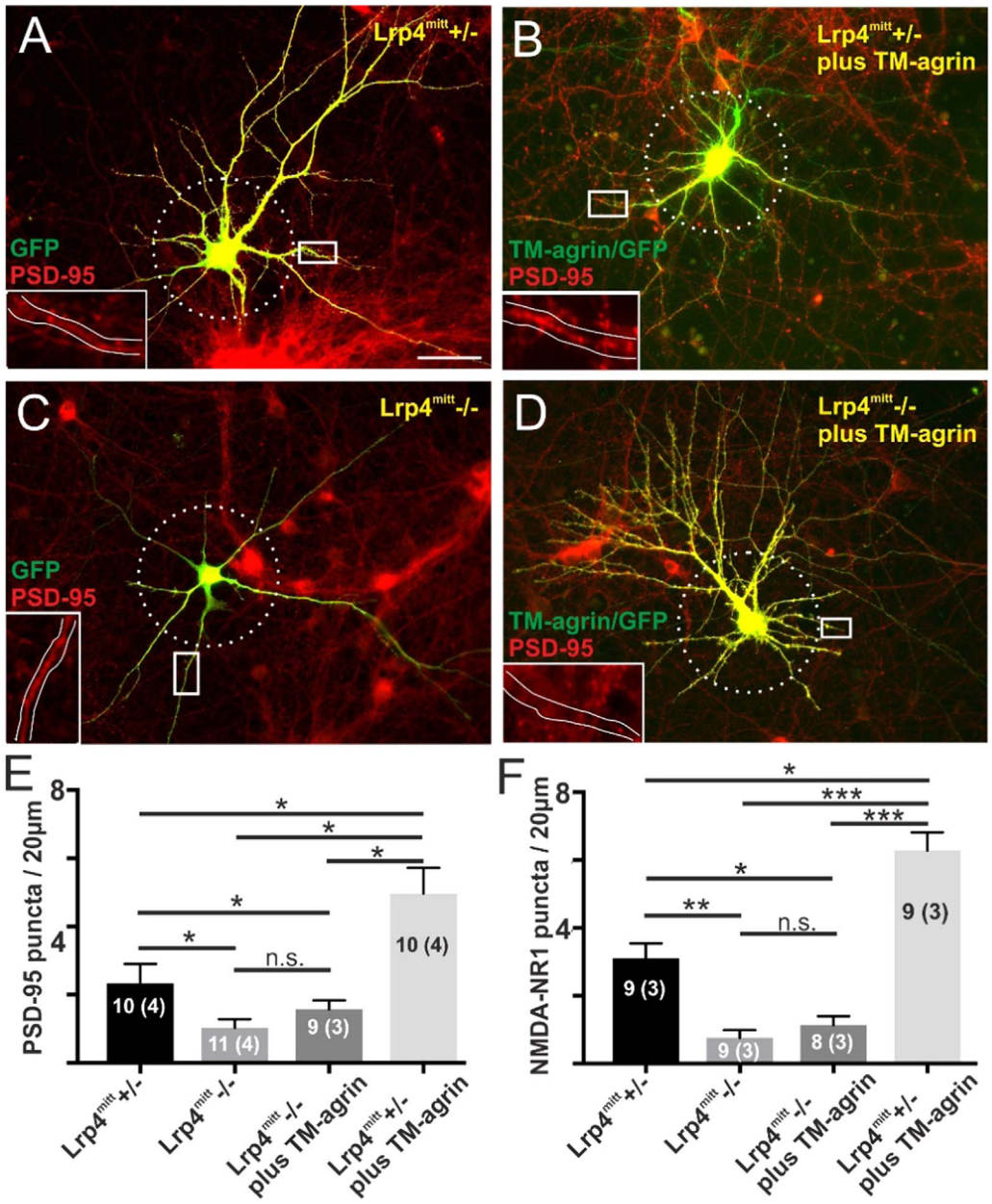

Fig. 2. Lrp4-deficient neurons have a reduced density of excitatory synaptic puncta and the reduction is ameliorated by TM-agrin transfection in neurons from heterozygous but not from homozygous Lrp4^{mitt} mice. Cortical neurons from heterozygous (A, B) and from homozygous Lrp4^{mitt} mice (C, D) were transfected at DIV 12 with a cDNA coding for mouse full-length TM-agrin (B, D) and stained at DIV14 with antibodies against PSD-95 (red channel). Higher magnification of the boxed areas in A–D are shown in the respective insets. The white lines in the insets outline the dendrite. Note the increased number of dendritic puncta containing PSD-95 in neurons from heterozygous but not in neurons from homozygous Lrp4^{mitt} mice transfected with TM-agrin (B, D). Quantification revealed that homozygous Lrp4^{mitt} mice have a reduced PSD-95 and NMDA receptor NR1 subunit puncta density compared to heterozygous littermate control mice (E, F). Transfection with TM-agrin increased the density of PSD-95 and NR1 subunit puncta in neurons from heterozygous (B, E, F) but not in neurons from homozygous Lrp4^{mitt} mice (D–F), suggesting that Lrp4 is required for the TM-agrin mediated increase in excitatory synaptic puncta. The dashed circle in panels A–D represents the radius of 50 µm outside of which the number of dendritic PSD-95 and NR1 subunit puncta was determined. The mean + SEM is shown in E and F. The Kruskal-Wallis Test with Dunn's correction for multiple comparison was applied. Numbers in columns represent the number of neurons (n) and, in parentheses, the number of animals (N) analyzed. Scale bar in A: 50 µm.

associated protein puncta as it had on the density of excitatory synapse-associated protein puncta, we first stained neurons from heterozygous or from homozygous Lrp4^{mitt} mice at DIV 14 with antibodies against gephyrin or against the α1-subunit of the $GABA_A$ receptor. We observed a decrease in the density of gephyrin and $GABA_A$ receptor puncta in neurons from homozygous Lrp4^{mitt} mice compared to neurons from heterozygous littermate controls (Fig. 3A, C), demonstrating that the expression of Lrp4 was required for the formation and/or maintenance of inhibitory synaptic puncta. Transfection of TM-agrin into cortical neurons from heterozygous Lrp4^{mitt} mice reduced the number of gephyrin and $GABA_A$ receptor puncta to a similar extent as in neurons from homozygous Lrp4^{mitt} mice (Fig. 3B, D–F and sup. Fig. S3). Transfection of TM-agrin into neurons from homozygous Lrp4^{mitt} mice did not further reduce the density of inhibitory synaptic puncta compared to neurons from homozygous Lrp4^{mitt} mice transfected with the control vector (Fig. 3C–F and sup. Fig. S3). Thus, inhibitory synapse density was reduced in neurons lacking Lrp4 as well as in control neurons transfected with TM-agrin. Since Lrp4 expression was not required for TM-agrin-induced reduction of inhibitory synapses, our results indicate independent mechanisms for the reduction of inhibitory synapses by overexpression of TM-agrin and by lack of Lrp4. In summary, our results demonstrate

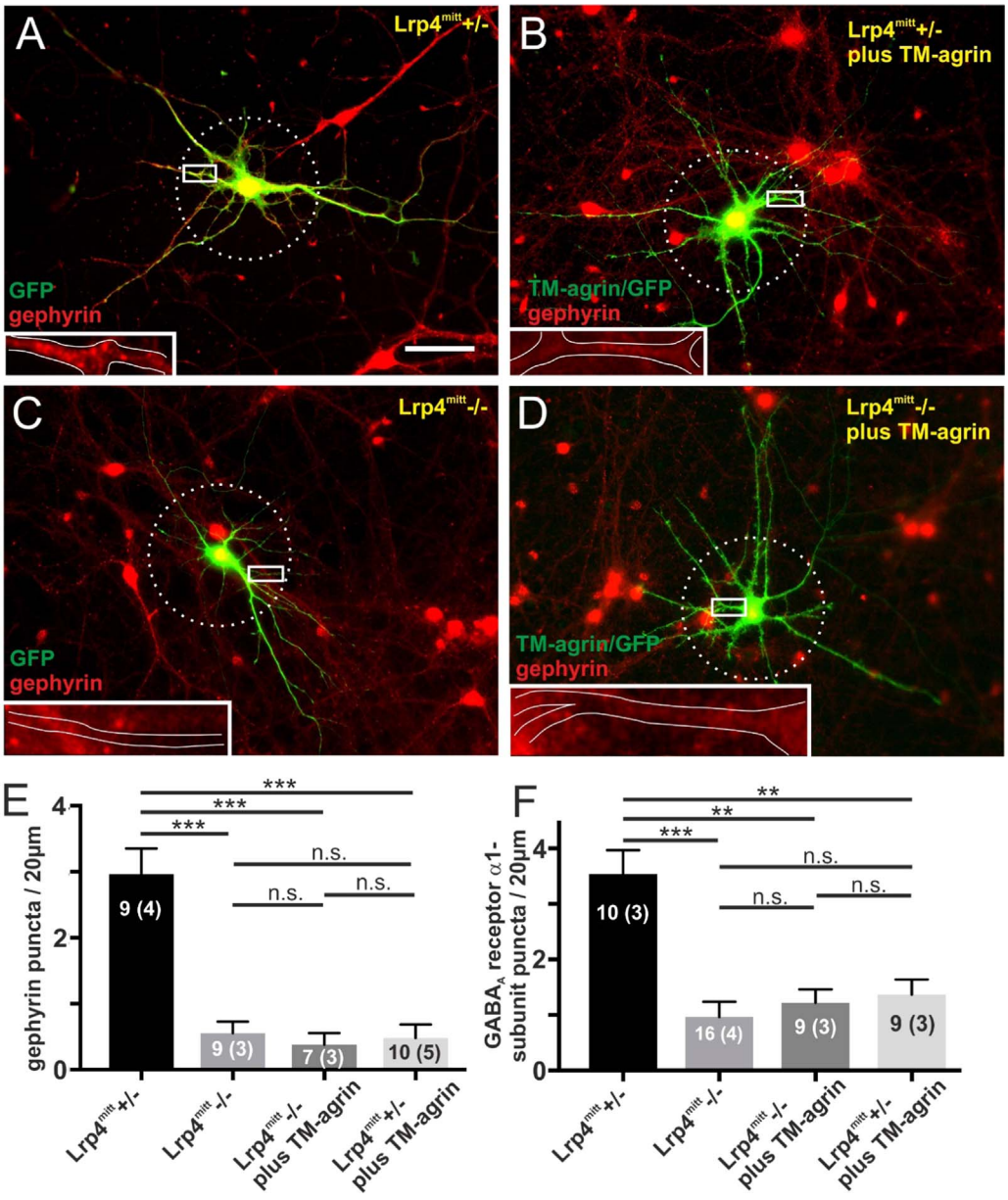

Fig. 3. Lrp4-deficient neurons and TM-agrin overexpressing neurons in culture have a reduced density of puncta of inhibitory synapse-associated proteins. Cortical neurons transfected with either the control plasmid coding for GFP (A, C) of with a cDNA coding for GFP plus full-length mouse TM-agrin (B, D) stained with antibodies against gephyrin (red channel in A–D) are shown. The insets in panels A–D show the boxed areas at higher magnification. Note that the number of gephyrin and of α1-subunit of the $GABA_A$ receptor puncta are reduced in neurons from homozygous $Lrp4^{mitt}$ mice compared to neurons from heterozygous control mice (E, F). Transfection of TM-agrin did not increase the number of gephyrin- or $GABA_A$ receptor α1 subunit puncta in neurons from heterozygous and homozygous $Lrp4^{mitt}$ mice (E, F). The mean + SEM is shown in panels E and F; Kruskal-Wallis-Test with Dunn's correction for multiple comparison. The dashed circle in panels A–D represents the radius of 50 µm inside of which the number of dendritic gephyrin and $GABA_A$ receptor α1 subunit puncta was determined. Numbers in columns represent the number of neurons (n) and, in parentheses, the number of animals (N) analyzed. Scale bar in A: 50 µm.

that Lrp4 expression is required for the formation of normal amounts of excitatory and inhibitory synapses. Moreover, transfection of cultured embryonic cortical neurons with TM-agrin cDNA differentially affected excitatory and inhibitory synapses. Overexpression of TM-agrin cDNA resulted in an Lrp4-dependent increase in the density of dendritic excitatory synaptic puncta and an Lrp4-independent decrease in the density of inhibitory synaptic puncta.

3.4. Expression of MuSK is required for normal dendritic arborization but not for the formation of synapse-like specializations

At the neuromuscular junction, agrin's synaptogenic effect is strictly dependent on the activation of the tyrosine kinase MuSK (DeChiara et al., 1996). To investigate if MuSK expression affects dendritic arborizations and the formation of synapses in the CNS, we analyzed embryonic neurons from MuSK-/- mice. We observed a reduced number of primary dendrites in neurons from MuSK-/- mice (Fig. 4B, D) compared to MuSK+/- mice (Fig. 4A, D). Likewise, quantification of the total dendritic branch tip number (Fig. 4E) as well as Sholl analysis (Fig. 4F) revealed a reduction in dendritic complexity in MuSK-/- mice compared to heterozygous littermate controls, demonstrating that MuSK expression is required for the formation of the normal dendritic branching pattern of embryonic CNS neurons. Transfection of full-length mouse TM-agrin cDNA into neurons from MuSK-/- mice did not affect any of the parameters characterizing dendritic complexity (Fig. 4C–F). Likewise, transfection of the TM-agrin cDNA into neurons from MuSK+/- mice did not change the dendritic branching compared to neurons from

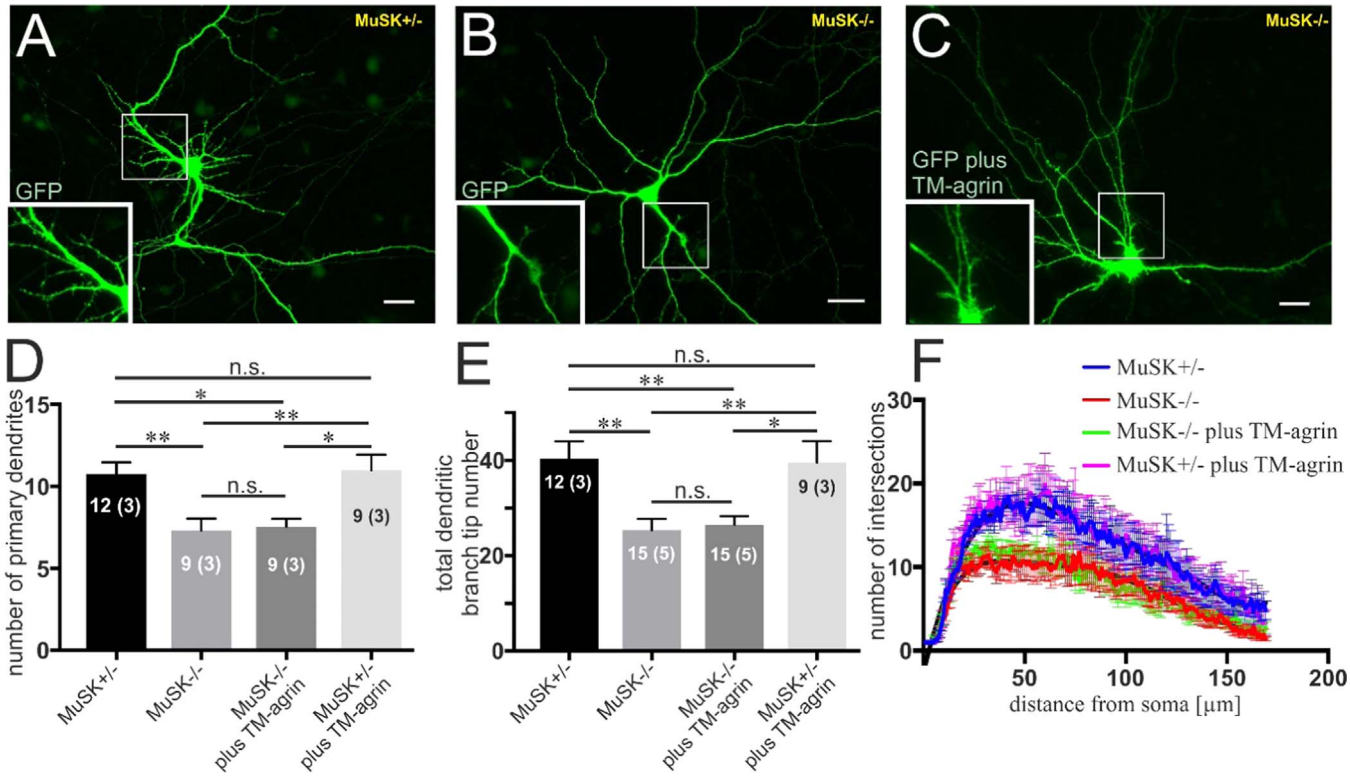

Fig. 4. MuSK expression is required for normal dendritic branching pattern. (A) Cortical neurons at DIV 14 from heterozygous (A) or homozygous (B, C) MuSK-deficient mice transfected at DIV12 with either a control vector coding for GFP (A, B) or a vector coding for GFP plus full-length mouse TM-agrin (C) are shown. Note the presence of filopodia-like protrusions in neurons transfected with the TM-agrin cDNA (inset in panel C). Quantification revealed that the number of primary dendrites (D), the total dendritic branch tip number (E) and the number of intersections determined by Sholl analysis (F) were reduced in neurons from homozygous MuSK-/- mice compared to heterozygous littermate controls. Transfection of TM-agrin cDNA into neurons from MuSK-/- mice did not increase the number of primary dendrites, total branch tip number and number of intersections, compared to neurons from MuSK+/- mice transfected with a control vector coding for GFP, demonstrating that expression of MuSK is required for agrin's effect on dendritic morphology. In addition, transfection of TM-agrin cDNA into neurons from MuSK+/- mice had no effect on the number of primary dendrites, number of intersections and total number of dendritic branch tips compared to neurons from MuSK+/- transfected with the control vector. Panels D–F show the mean + SEM. Numbers in columns represent the number of neurons (n) and, in parentheses, the number of animals (N) analyzed. Statistical analysis was performed using the one-way ANOVA test with Tukey's correction for multiple comparison. Scale bar in panels A–C: 50 µm.

MuSK +/- mice transfected with the control vector (Fig. 4D–F). Thus, TM-agrin transfection restored normal dendritic branching patter in Lrp4-deficient neurons, but did not ameliorate the reduced dendritic complexity in MuSK-deficient neurons.

Next, we explored if MuSK expression affected the formation or maintenance of excitatory and inhibitory synapses. We detected no difference in the density of puncta labeled with antibodies against PSD-95 in neurons from MuSK-/- mice compared to MuSK heterozygous littermate controls (sup. Fig. S4A–D). Likewise, we observed no change in the density of puncta labeled with antibodies against gephyrin (sup. Fig. S5A–D) or against the α1-subunit of the $GABA_A$ receptor (sup. Fig. S5E) in MuSK-/- mice compared to MuSK+/- control mice. Moreover, transfection of TM-agrin induced an increase in the density of dendritic PSD-95 puncta (sup. Fig. S4C, D) and a decrease in the density of gephyrin puncta (sup. Fig. S5C, D) and of the α1-subunit of the $GABA_A$ receptor (sup. Fig. S5E) independent of MuSK expression. Collectively, these results demonstrate that MuSK expression is necessary for the normal dendritic arborization pattern but not for the formation of excitatory or inhibitory synapses. Moreover, MuSK appears not to be required for agrin's effect on the density of excitatory or inhibitory synapses.

3.5. Soluble agrin induces an increase in the frequency and amplitude of mEPSCs of cortical neurons in microisland cultures

The TM-agrin-induced increase in PSD-95/NR1 puncta and the decrease in gephyrin/α1-$GABA_A$ receptor puncta density suggested an effect of agrin on the formation or maintenance of excitatory and inhibitory synapses. To test this hypothesis, we used electrophysiological methods and investigated whether agrin influenced the formation of functional synapses. To this end, we cultured individual cortical neurons prepared from E15 C57BL/6N wildtype mouse embryos on a pre-formed and physically restricted astrocytic microisland to promote the formation of autapses (Fig. 5A). This culture system is suitable for investigating basic mechanisms of synaptic transmission and at the same time avoids neuronal network activity. After 12–15 days *in vitro* all neurons were synaptically active as determined by whole cell patch clamp recordings (sup. Fig. S6A). Approximately 66.5% of the individual neurons were excitatory and 33.5% were inhibitory as determined by the decay kinetics of the mPSCs (sup. Fig. S6B; Rost et al., 2010). Thus, excitatory and inhibitory synapses could be investigated independently in this culture system.

To analyze if the number of synapses was affected by agrin or Lrp4, we determined the frequency and amplitude of spontaneous mEPSC and mIPSC currents of cortical neurons in microisland cultures using whole-cell patch-clamp recordings in the presence of TTX (1 µM) to block generation of action potentials. The frequency of the mEPSCs increased with prolonged culturing (sup. Fig. S6C), whereas the mIPSCs frequency was the highest at DIV 10–11 and slightly declined at DIV 12–15 (sup. Fig. S6C). mEPSCs could be blocked completely by DNQX (20 µM) and APV (100 µM; sup. Fig. S6D), demonstrating that they were mediated by glutamate receptors. mIPSCs could be blocked completely by bicuculline (20 µM; sup. Fig. S6E), suggesting that they are derived from $GABA_A$ receptor-mediated synaptic transmission.

Since we were not able to reliably transfect individual neurons in the microisland cultures, we applied soluble agrin to investigate its

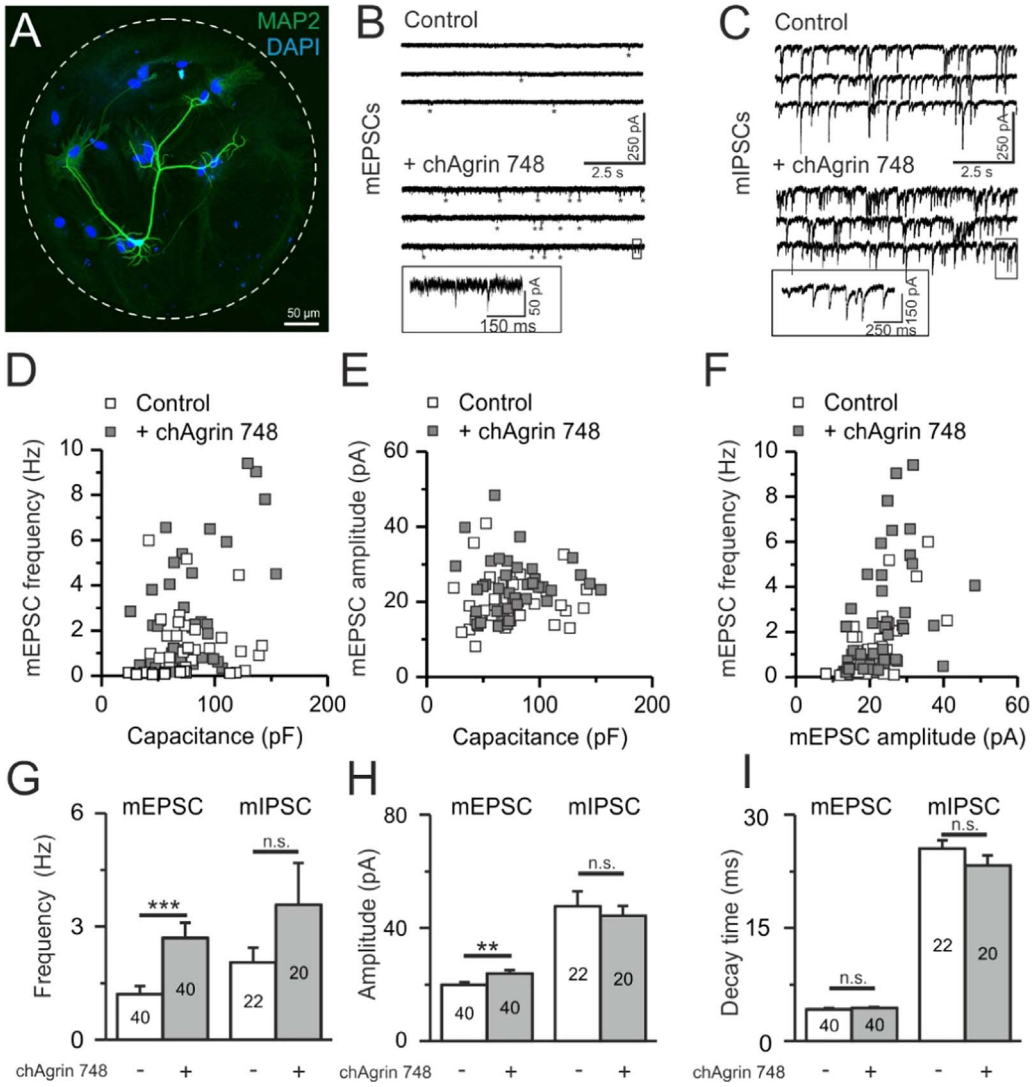

Fig. 5. Agrin induces a selective increase in the frequency of mEPSCs but not of mIPSCs in cultured cortical neurons. Panel A shows a representative single neuron (labeled by antibodies against MAP2; green channel) on an astrocyte layer (stained by DAPI; blue channel). The dashed white circle delineates the boundaries of the microisland. Addition of purified full-length chick agrin to cultures of wildtype neurons resulted in an increase in mEPSC frequency (B and G) and mEPSC amplitude (H). In contrast, frequency and amplitude of mIPSCs were not affected by the agrin incubation (C, G, H). In contrast to the frequency and amplitude, the decay time constants of mEPSCs and mIPSCs were not affected (I). Correlations between mEPSC frequency or amplitude with capacitance were analyzed in D and E, respectively. In panel F the correlation between mEPSC frequency and amplitude was analyzed. p-values were determined by the Mann-Whitney rank sum test or the paired *t*-test. Numbers in columns in G–I correspond to the number of cells analyzed. Bar plots represent mean + SEM. mEPSCs and mIPSCs were recorded at a holding potential of – 70 mV in the presence of TTX.

effect on the electrophysiological properties of cortical neurons. Application of soluble full-length chick agrin (isoform A4B8) purified from HEK293 culture supernatants (sup. Fig. S6F; Bezakova et al., 2001) at a concentration of 1 µg/ml for 3–5 h doubled the frequency of mEPSCs of single wildtype cortical neurons (Fig. 5A, B, D, G). Moreover, the amplitude of the mEPSCs increased from 19.93 ± 1.0 (N = 40 cells) to 23.95 ± 1.2 pA (N = 40 cells; Fig. 5E, H) while the decay time constant and the rise time (10–90%) remained unaffected (Fig. 5I). The frequency (Fig. 5C, G), amplitude (Fig. 5C, H) and the decay time (Fig. 5I) of mIPSCs were not different in cultures from wildtype neurons treated with agrin compared to similar cultures without agrin addition, suggesting that soluble agrin had no effect on inhibitory synapses in the microisland cultures. Correlating mEPSC frequency and amplitude with the respective capacitance of the cell (as a measure of cell size, see sup. Fig. S9) did not reveal an inter-dependency of these synaptic properties on each other (Fig. 5D). The mEPSC frequencies also did not correlate with the amplitude of the events (Fig. 5E, F). These results demonstrate that incubation of wildtype neurons with soluble agrin selectively increased excitatory postsynaptic current frequency and amplitude but had little, if any, effect on the electrophysiological properties of inhibitory synapses.

The agrin-mediated increase of the amplitude and frequency of mEPSCs suggested either a selective increase of excitatory synapse numbers, changes of postsynaptic receptor densities and/or a change in the presynaptic neurotransmitter release properties. To distinguish between these possibilities, paired-pulse recordings were analyzed, a commonly used approach to determine the presynaptic function (Zucker and Regehr, 2002). As single neurons were used in this study that reliably formed autaptic connections, paired pulse experiments could be performed by briefly raising the membrane potential of the investigated neuron to 0 mV for 1 ms at 100 ms intervals to elicit autaptic EPSCs (aEPSCs). In the presence of agrin, we observed an increase in the amplitude of the evoked EPSCs (Fig. 6A, C) as well as an increase in the quantal content of the neurons (Fig. 6F) compared to neurons not treated with agrin. Using an inter stimulus interval of 100 ms, no change in the paired pulse ratio was observed after

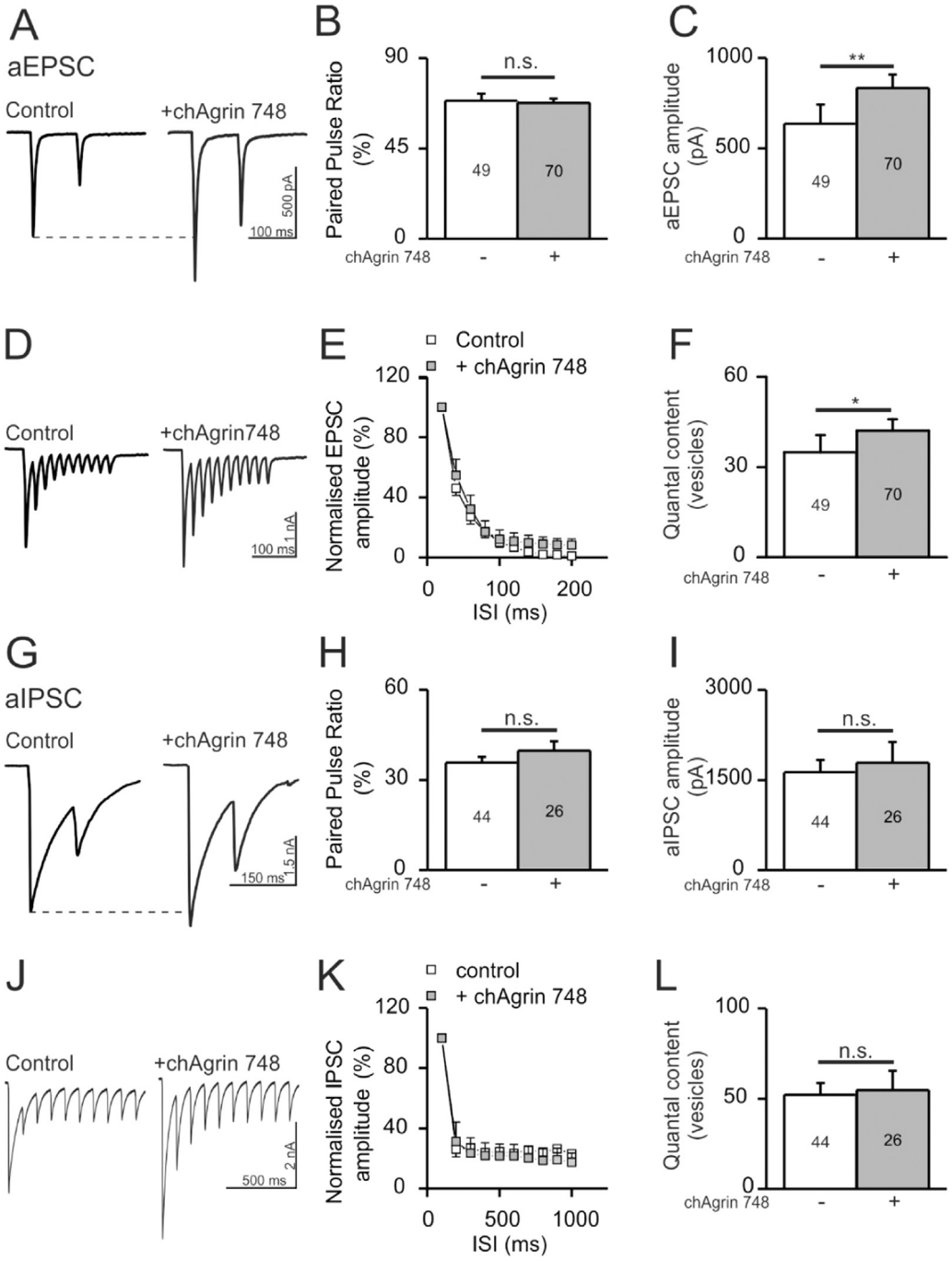

Fig. 6. Incubation of cortical neurons in microisland cultures with agrin does not alter presynaptic parameters of excitatory or inhibitory neurons. Both evoked EPSCs of control and agrin-treated neurons showed paired-pulse depression (A) but did not differ from each other in their paired-pulse ratio (B) even though an increase of evoked autaptic amplitude (C) and quantal content (F) was measured. Quantal content represents an average value of different synapses from an individual neuron (for details see Materials and Method section). High frequency stimulation also did not show differences in neurotransmitter release between agrin-treated and untreated neurons (D, E). Agrin-treated inhibitory neurons showed no difference in paired-pulse ratio compared to untreated neurons (G, H). All neurons showed depression as indicated by single traces (A) and no changes in evoked autaptic amplitudes (I) or the quantal content (L). In addition, high frequency stimulation did not reveal differences in neurotransmitter release between agrin treated and untreated neurons (J, K). Statistical analysis was done using Mann-Whitney rank sum tests. Numbers in columns represent individual cells measured. Bars represent mean values + SEM. Evoked autaptic excitatory synaptic currents (aEPSCs) and evoked autaptic inhibitory synaptic currents (aIPSCs) were recorded at a holding potential of – 70 mV.

incubation with soluble agrin (Fig. 6B). All investigated cells displayed a paired pulse depression indicative of a high release probability of neurotransmitter. High frequency stimulation at 50 Hz did not reveal differences in neurotransmitter release between excitatory neurons with or without added agrin (Fig. 6D, E). These data demonstrate that incubation of wildtype neurons with soluble agrin did not apparently alter presynaptic functions at excitatory synapses.

Autaptic stimulation of inhibitory neurons at an inter stimulus interval of 100 ms revealed none of the changes observed for excitatory neurons. The amplitude of the evoked IPSCs or the quantal content of the mIPSCs was not affected by agrin incubation (Fig. 6 G, I, L). All cells investigated displayed paired pulse depression as was observed in the evoked EPSCs (Fig. 6G, H). High frequency stimulation at 10 Hz likewise did not reveal changes in the release of neurotransmitter

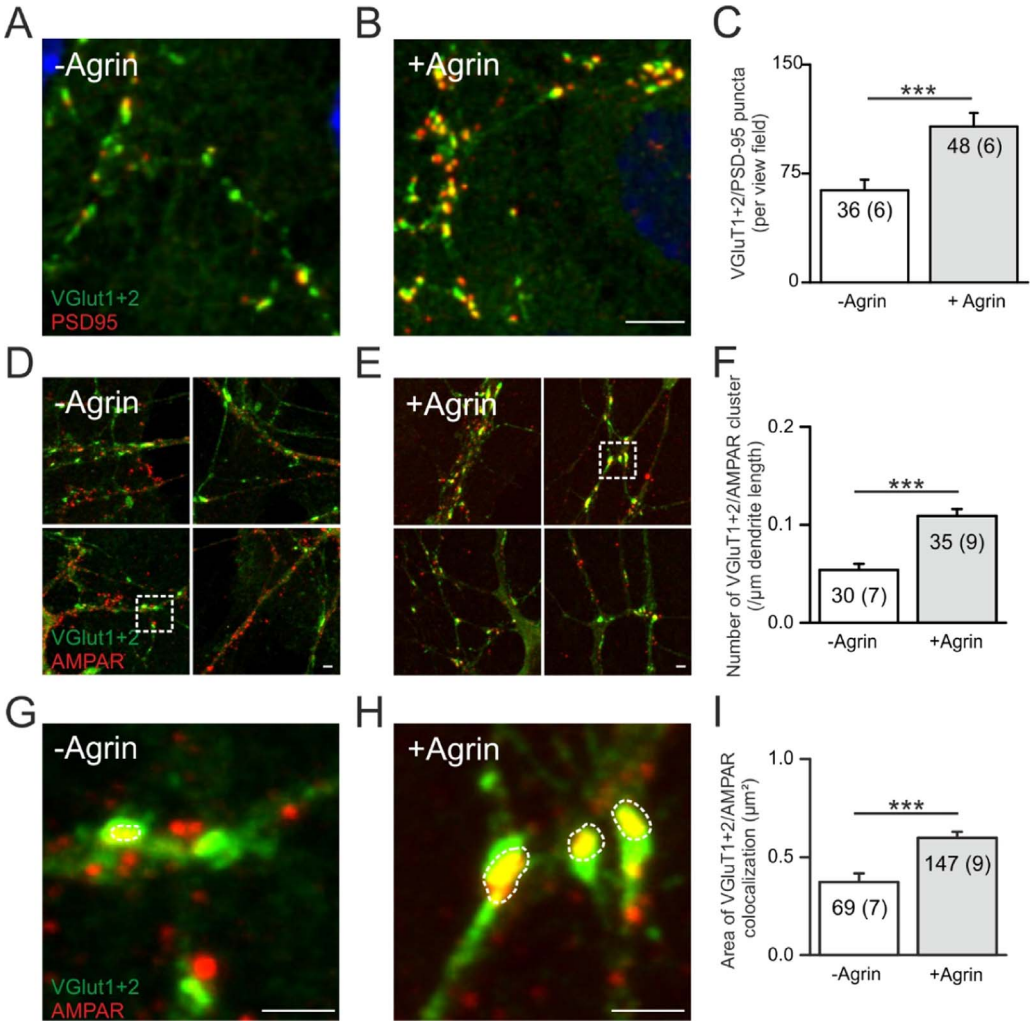

Fig. 7. Agrin increased the number of and the area of synaptic PSD-95 and AMPA receptor clusters. Microisland cultures were stained with antibodies against PSD-95 and VGlut1+2 (A–C) or anti-AMPA receptor and VGluT1+2 (D, E, G, H). An increase in the number of puncta with VGlut1+2 immunoreactivity colocalizing with anti-PSD-95 or anti-AMPA receptor antibodies was observed in the presence of agrin (C, F). Numbers in columns represent numbers of dendrites (n) and the number of individual neurons (N) that were analyzed. The area of AMPA receptors and colocalized VGlut1+2 immunoreactivity increased in agrin-treated neurons compared to control neurons (G, H, I). Panels G and H show higher magnifications of the dashed boxes in D and E, respectively. Adding agrin led to a significant increase in AMPA receptor cluster area (I). The same cells were used for the data evaluation in I as in F. Numbers in columns represent the number of AMPA receptor clusters (n) and in parenthesis the number of individual neurons (N) analyzed. Bar represent mean values + SEM. Statistical analysis was performed using the Mann-Whitney rank sum test. Scale bars: 5 µm.

(Fig. 6J, K). Collectively, these data strongly suggest that soluble agrin did not induce presynaptic changes in excitatory or inhibitory neurons in the microisland culture system.

3.6. Agrin increases the number and the size of glutamatergic synaptic puncta

In the absence of any presynaptic changes, the agrin-dependent increase in the mEPSC frequency and amplitude suggested either an increased number of synapses or changes of postsynaptic receptor densities as the underlying mechanism. To investigate these possibilities, the number of synaptic puncta in neurons in the microisland cultures was determined immunocytochemically using antibodies to simultaneously label pre- and postsynaptic marker proteins of glutamatergic synapses (VGlut1+2 and PSD-95). We observed a 2-fold increase in synaptic puncta number in agrin-treated cultures compared to untreated control neurons (Fig. 7A–C). Similar results were obtained using antibodies against the AMPA receptor and against VGlut1+2 (Fig. 7D–F). Furthermore, analysis of the area covered by clustered AMPA receptors in the presence or absence of soluble agrin revealed a 2-fold increase of the area in which the immunoreactivity of both markers overlapped in neurons treated with agrin compared to untreated neurons (Fig. 7G–I). These results support the hypothesis that the agrin-dependent increase of the amplitude and frequency of mEPSCs (Fig. 5B, G, H) was mediated by an increased number of functional glutamatergic synapses and the incorporation and/or recruitment of AMPA receptors into the postsynaptic membrane.

3.7. Lrp4 expression is essential for the agrin-induced increase in mEPSCs

To determine if the agrin-mediated increase in the amplitude and frequency of mEPSCs depended on the expression of Lrp4, we analyzed the electrophysiological properties of Lrp4-deficient cortical neurons in microisland cultures in the presence and absence of soluble agrin. In contrast to wild type mice, application of soluble full-length chick agrin to neurons from Lrp4 knockout mice did not result in an increase in mEPSC frequency (Fig. 8A, B) or amplitude (Fig. 8A, C). These results demonstrate that in microisland cultures Lrp4 is essential for the agrin-mediated increase in cortical neuron excitatory synapse density. As expected, no change in mIPSC frequency and amplitude was detected in the absence of Lrp4 and after incubation with soluble agrin

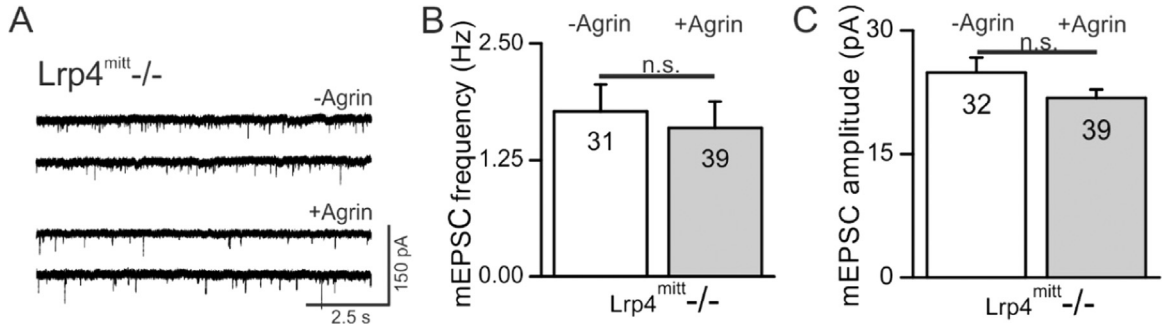

Fig. 8. Analysis of the synaptic properties of Lrp4-deficient neurons. Voltage clamp traces at − 70 mV holding potential show that Lrp4-deficient neurons form functional synapses as can be seen by the recorded mEPSCs (A). Incubation with soluble agrin did not increase the frequency of these events (B). The amplitudes of these events stayed on a similar level after adding agrin (C). Statistical significance was tested using Mann-Whitney rank sum tests. Numbers in columns in B to C represent individual cells investigated. Bar plots represent means + SEM. mEPSCs were recorded in presence of TTX.

(mean mIPSC frequency without agrin: 0.42 ± 0.118; n = 8; in the presence of soluble agrin: 0.56 ± 0.181; n = 8. Mean amplitude without agrin: 27.52 ± 5; n = 8; in the presence of soluble agrin: 31.1 ± 2.9; n = 8).

Collectively, the electrophysiological and immunocytological data obtained from the microisland cultures confirm our observations in standard monolayer cultures regarding the effect of Lrp4 and TM-agrin on the density of PSD-95 puncta. Both types of experimental approaches suggest that Lrp4 and agrin cooperate during the formation or maintenance of excitatory synapses *in vitro*.

4. Discussion

Several lines of evidence have demonstrated the essential role of agrin, MuSK and Lrp4 during formation, maintenance and regeneration of the NMJ (for review see Tintignac et al., 2015). In contrast, the role of these molecules in the developing CNS is much less clear. In particular, the putative cooperation of agrin with Lrp4 and MuSK at developing central nervous system synapses has not been analyzed. Due to the perinatal lethality of Lrp4-, MuSK- or agrin-deficient mice, direct examination of the role of these three components during synapse formation in the CNS appears difficult (Gautam et al., 1996; DeChiara et al., 1996; Weatherbee et al., 2006). However, cultures of embryonic cortical or hippocampal neurons develop excitatory and inhibitory synapses that appear functionally similar to those formed by wildtype neurons (Serpinskaya et al., 1999; Li et al., 1999). Therefore, we analyzed the function of agrin, MuSK and Lrp4 in two different cell culture systems using embryonic neurons from Lrp4- and MuSK mutant mice in combination with the transfection or addition of agrin. We show that agrin, MuSK and Lrp4 cooperate differentially during synaptic differentiation and dendritic tree development. In the absence of Lrp4, but not in the absence of MuSK, embryonic cortical neurons have a reduced density of excitatory and inhibitory synaptic specializations. Overexpression of TM-agrin in cultured wildtype but not in Lrp4-deficient neurons increased the number of excitatory synapses, suggesting that the effect of TM-agrin is dependent on Lrp4 expression. Thus, a selective functional cooperation of agrin and Lrp4 appears possible during the formation of excitatory synapses. In this experimental setting, MuSK was not required for the TM-agrin-induced increase of excitatory synapses.

Interestingly, we observed a severe reduction of the density of dendritic aggregates containing gephyrin or the $GABA_A$ receptor α1-subunit after transfection with TM-agrin in cultures of wildtype cortical neurons. This effect was independent of the presence of MuSK. Whether Lrp4 expression was required for this reduction could not be evaluated since no further decrease was detected after TM-agrin transfection of Lrp4-deficient neurons compared to neurons from wild type mice transfected with TM-agrin. In a previous study, treatment of embryonic rat hippocampal neurons in monolayer cultures with soluble agrin increased the $GABA_A$ receptor cluster size and mIPSC amplitude but not mIPSC frequency (Pribiag et al., 2014). In contrast, we were not able to detect an effect of soluble agrin on mIPSC frequency and amplitude in microisland cultures. Similarly, agrin has been colocalized with gephyrin in cultured retinal neurons (Mann and Kröger, 1996) and in cultured embryonic rat hippocampal neurons (Pribiag et al., 2014). In contrast, agrin did not appear to be concentrated at inhibitory synapses in the CNS and the frequency and amplitude of mIPSCs was not affected in cortical neurons from agrin-deficient brains *in vivo* (Ksiazek et al., 2007). One potential explanation for these differences could be that *in vivo* adult neurons were analyzed, in contrast to the embryonic neurons analyzed in the *in vitro* studies. Alternatively, compensatory effects *in vivo* might have obscured an acute effect of agrin. Moreover, different agrin isoforms or differential effects of soluble agrin on inhibitory synapses in monolayer cultures compared to microisland cultures might contribute to the differences observed in the various studies. In any case, our data demonstrate opposing effects of TM-agrin overexpression on glutamatergic and GABAergic synapses.

To further substantiate the effect of agrin on the formation or maintenance of excitatory and inhibitory synapses, we used microisland cultures and investigate the effect of agrin on neurons expressing or lacking Lrp4. This culture system allowed the selective analysis of individual excitatory or inhibitory neurons and, thus, lacks any potentially interfering neuronal network activity. This appeared important since for example electrophysiological analysis of Lrp4-deficient neurons in monolayer culture did not reveal electrophysiological changes compared to wildtype neurons (Karakatsani et al., 2017). After incubation with soluble agrin, neurons from wildtype mice showed a significant increase in the frequency and amplitude of mEPSCs and of evoked EPSCs as well as of the size of excitatory synaptic puncta. In contrast, adding soluble agrin to Lrp4-deficient neurons did not induce an increase in mEPSC frequency or in dendritic excitatory synaptic puncta. These results demonstrate that agrin's effect on excitatory synapses required the expression of Lrp4 and are in line with the transfection experiments of TM-agrin in Lrp4-deficient neurons. The frequency of mIPSCs was not affected by soluble agrin in the microisland culture. Again, this indicates that the multidomain protein agrin has distinct functions on CNS neurons, which might be executed by different domains within agrin and in cooperation with distinct interaction partners including MuSK or Lrp4.

We also demonstrate a requirement of Lrp4 and MuSK expression during establishment of the dendritic branching pattern in cultured cortical neurons. In the absence of Lrp4 or MuSK dendritic branching was impaired, supporting our previous studies using synthetic microRNAs *in vitro* as well as *in vivo* to knockdown Lrp4 (Karakatsani et al., 2017). In contrast, an altered dendritic arborization pattern was not observed in Lrp4-deficient cortical or hippocampal neurons *in vivo* (Sun et al., 2016). The results from the present study

now demonstrate that synthetic miRNA-mediated knockdown of Lrp4 and genetic ablation of Lrp4 expression lead to similar dendritic phenotypes in cultured neurons and might suggest that compensatory mechanisms are activated *in vivo* to restore or maintain normal dendritic branching pattern in Lrp4-deficient neurons. Interestingly, in the present study the dendritic branching deficit in Lrp4-deficient neurons could be compensated by overexpression of TM-agrin suggesting that Lrp4 is not required for TM-agrin's effect on the dendritic morphology. In contrast, we observed no compensatory effect of TM-agrin overexpression on the dendritic arborization patter of MuSK-deficient neurons. Thus, agrin, Lrp4 and MuSK might functionally cooperate during formation of the normal dendritic morphology. It is currently not known whether TM-agrin and Lrp4 directly interact on cortical neurons to modulate dendritic morphologies. However, TM-agrin transfected 293HEK cells are able *in vitro* to induce aggregation of AChRs at the contact site between the myotubes and the HEK cells, suggesting that both proteins are in principle able to directly interact (Neumann et al., 2001). Our results regarding TM-agrin overexpression and addition of soluble agrin to wildtype, Lrp4- or MuSK-deficient neurons on dendritic branching as well as synapse formation are summarized in Supplementary Table 1.

Several mouse mutants of Lrp4 have been generated to unravel the function of Lrp4 in the brain (Gomez et al., 2014; Pohlkamp et al., 2015; Sun et al., 2016). The overall brain structure in these mutant mice appeared normal, but the spine density on CA1 neurons was reduced (Sun et al., 2016; Gomez et al., 2014) while dendritic arborization appeared not to be affected (Sun et al., 2016). Moreover, adult mice with Lrp4-deficient brains show profound deficits in cognitive tasks that accessed learning and memory (Gomez et al., 2014). In these studies, it was shown that the Lrp4 mutants have deficits in LTP and a reduced mEPSC frequency. The latter parallels observations on a reduced mEPSC frequency made in adult agrin-deficient brains from mice in which the perinatal lethality and defective NMJ development was rescued by reexpression of mini-agrin selectively in motoneurons (Ksiazek et al., 2007). Likewise, knockdown of agrin expression using an RNAi lentivirus reduced excitatory synapse density along hippocampal dendrites (McCroskery et al., 2009). These studies collectively suggest a functional cooperation of agrin and Lrp4 during formation of excitatory synapses in the CNS. However, different observations in Lrp4 mutants were made regarding the mechanism of the synaptic changes due to Lrp4 deficiency. Two studies were unable to detect deficits in the presynaptic function in Lrp4-deficient neurons (Gomez et al., 2014; Pohlkamp et al., 2015), while another study revealed deficits in the presynaptic functions (increased paired pulse ratio; Sun et al., 2016). In the latter study, it was demonstrated that agrin affected the efficacy of glutamatergic synaptic transmission of CA1 pyramidal neurons in the mature hippocampus by modifying nucleotide release from astrocytes *via* astrocytic Lrp4 expression (Sun et al., 2016). ATP released from astrocytes is converted to adenosine that activates adenosine A1 receptors in glutamatergic presynapses. Consistent with these observations were electrophysiological recordings of Lrp4-deficient hippocampal CA1 neurons that demonstrated increased paired-pulse ratios indicative for an altered presynaptic function (Sun et al., 2016). In the present study, astrocytes were present in both types of cultures raising the possibility that the effects on the formation or stabilization of synaptic puncta or the increased mEPSC frequency might be indirectly generated by agrin through interaction with Lrp4 on astrocytes. However, several lines of evidence make this unlikely. In the study by Sun et al. mature hippocampal synapses were investigated that were encapsulated by astrocytic processes. In their recordings exclusively presynaptic functions of Lrp4 and agrin were detected. In contrast, in our study we used cortical neurons from embryonic day 15 and, importantly, agrin-induced effects in the microisland cultures were clearly restricted to the postsynapse. The analysis of repetitive stimulation and paired-pulse ratios excluded a presynaptic effect of Lrp4 and agrin in these embryonic cortical neurons. Moreover, the embryonic neurons displayed paired-pulse depression indicative of a high release probability of the neurotransmitter, whereas the adult neurons investigated by Sun et al. revealed synaptic facilitation. Thus, our data strongly support the hypothesis that in embryonic neurons soluble agrin affects excitatory synapses *via* neuronal Lrp4 rather than *via* astrocytes.

In summary, our results suggest that agrin and Lrp4 functionally interact directly or indirectly and that this interaction is required for the formation of excitatory synapses. Agrin does not require MuSK for its effect on synapse density. Furthermore, agrin's effect on the development of the complexity of dendritic arborizations is independent of Lrp4 but might require MuSK. It should be noted, however, that in all studies analyzing the role of agrin in the CNS, only approximately 30% of the synapses were affected (Ksiazek et al., 2007; this study). It remains to be determined if these synapses represent a specific subpopulation, or if compensatory mechanisms are effective that limit the effect of agrin and Lrp4 in neurons.

Acknowledgements

We thank A. Hammes-Lewin (MDC) for providing the Lrp4 mutant mice, M. Rüegg (Biocenter Basel) for the MuSK knockout mice, K. Bach, A. Banerjee, M. Henning and I. Vitali for expert technical assistance. We are grateful to David Petrik for critical reading of the manuscript, C. Rosenmund and A. Felies (Charité, Berlin, Germany) for help preparing cortical microisland cultures.

Funding

This work was supported by DFG Grants SFB665 and Ra 424/5-1 to FGR.

Declarations of interest

None.

Appendix A. Supplementary material

Supplementary data associated with this article can be found in the online version at doi:10.1016/j.ydbio.2018.10.017.

References

Bezakova, G., Helm, J.P., Francolini, M., Lomo, T., 2001. Effects of purified recombinant neural and muscle agrin on skeletal muscle fibers in vivo. J. Cell Biol. 153, 1441–1452.

Brewer, G.J., Torricelli, J.R., Evege, E.K., Price, P.J., 1993. Optimized survival of hippocampal neurons in B27-supplemented Neurobasal, a new serum-free medium combination. J. Neurosci. Res. 35, 567–576.

Burgess, R.W., Skarnes, W.C., Sanes, J.R., 2000. Agrin isoforms with distinct amino termini: differential expression, localization, and function. J. Cell Biol. 151, 41–52.

Burk, K., Desoeuvre, A., Boutin, C., Smith, M.A., Kröger, S., Bosio, A., Tiveron, M.C., Cremer, H., 2012. Agrin-signaling is necessary for the integration of newly generated neurons in the adult olfactory bulb. J. Neurosci. 32, 3759–3764.

Daniels, M.P., 2012. The role of agrin in synaptic development, plasticity and signaling in the central nervous system. Neurochem. Int. 61, 848–853.

de Wit, J., Ghosh, A., 2016. Specification of synaptic connectivity by cell surface interactions. Nat. Rev. Neurosci. 17, 22–35.

DeChiara, T.M., Bowen, D.C., Valenzuela, D.M., Simmons, M.V., Poueymirou, W.T., Thomas, S., Kinetz, E., Compton, D.L., Rojas, E., Park, J.S., Smith, C., Distefano, P.S., Glass, D.J., Burden, S.J., Yancopoulos, G.D., 1996. The receptor tyrosine kinase MuSK is required for neuromuscular junction formation in vivo. Cell 85, 501–512.

Eusebio, A., Oliveri, F., Barzaghi, P., Ruegg, M.A., 2003. Expression of mouse agrin in normal, denervated and dystrophic muscle. Neuromuscul. Disord. 13, 408–415.

Falo, M.C., Reeves, T.M., Phillips, L.L., 2008. Agrin expression during synaptogenesis induced by traumatic brain injury. J. Neurotrauma 25, 769–783.

Ferreira, T.A., Blackman, A.V., Oyrer, J., Jayabal, S., Chung, A.J., Watt, A.J., Sjostrom, P.J., van Meyel, D.J., 2014. Neuronal morphometry directly from bitmap images. Nat. Methods 11, 982–984.

Fuerst, P.G., Rauch, S.M., Burgess, R.W., 2007. Defects in eye development in transgenic

mice overexpressing the heparan sulfate proteoglycan agrin. Dev. Biol. 303, 165–180.
Garcia-Osta, A., Tsokas, P., Pollonini, G., Landau, E.M., Blitzer, R., Alberini, C.M., 2006. MuSK expressed in the brain mediates cholinergic responses, synaptic plasticity, and memory formation. J. Neurosci. 26, 7919–7932.
Gautam, M., DeChiara, T.M., Glass, D.J., Yancopoulos, G.D., Sanes, J.R., 1999. Distinct phenotypes of mutant mice lacking agrin, MuSK, or rapsyn. Dev. Brain Res. 114, 171–178.
Gautam, M., Noakes, P.G., Moscoso, L., Rupp, F., Scheller, R.H., Merlie, J.P., Sanes, J.R., 1996. Defective neuromuscular synaptogenesis in agrin-deficient mutant mice. Cell 85, 525–535.
Gomez, A.M., Froemke, R.C., Burden, S.J., 2014. Synaptic plasticity and cognitive function are disrupted in the absence of Lrp4. eLife 3, e04287.
Henneberger, C., Juttner, R., Rothe, T., Grantyn, R., 2002. Postsynaptic action of BDNF on GABAergic synaptic transmission in the superficial layers of the mouse superior colliculus. J. Neurophysiol. 88, 595–603.
Ippolito, D.M., Eroglu, C., 2010. Quantifying synapses: an immunocytochemistry-based assay to quantify synapse number. J. Vis. Exp.. http://dx.doi.org/10.3791/2270.,2270.
Karakatsani, A., Marichal, N., Urban, S., Kalamakis, G., Ghanem, A., Schick, A., Zhang, Y., Conzelmann, K.K., Ruegg, M.A., Berninger, B., Ruiz de Almodovar, C., Gascon, S., Kroger, S., 2017. Neuronal LRP4 regulates synapse formation in the developing CNS. Development 144, 4604–4615.
Kim, N., Stiegler, A.L., Cameron, T.O., Hallock, P.T., Gomez, A.M., Huang, J.H., Hubbard, S.R., Dustin, M.L., Burden, S.J., 2008. Lrp4 is a receptor for Agrin and forms a complex with MuSK. Cell 135, 334–342.
Klenowski, P.M., Fogarty, M.J., Belmer, A., Noakes, P.G., Bellingham, M.C., Bartlett, S.E., 2015. Structural and functional characterization of dendritic arbors and GABAergic synaptic inputs on interneurons and principal cells in the rat basolateral amygdala. J. Neurophysiol. 114, 942–957.
Koulen, P., Honig, L.S., Fletcher, E.L., Kröger, S., 1999. Expression, distribution and ultrastructural localization of the synapse-organizing molecule agrin in the mature avian retina. Eur. J. Neurosci. 11, 4188–4196.
Kröger, S., Pfister, H., 2009. Agrin in the nervous system – synaptogenesis and beyond. Future Neurol. 4, 67–86.
Ksiazek, I., Burkhardt, C., Lin, S., Seddik, R., Maj, M., Bezakova, G., Jucker, M., Arber, S., Caroni, P., Sanes, J.R., Bettler, B., Ruegg, M.A., 2007. Synapse loss in cortex of agrin-deficient mice after genetic rescue of perinatal death. J. Neurosci. 27, 7183–7195.
Li, L., Xiong, W.C., Mei, L., 2018. Neuromuscular junction formation, aging, and disorders. Ann. Rev. Physiol. 80, 159–188.
Li, Z., Hilgenberg, L.G.W., O'Dowd, D.K., Smith, M.A., 1999. Formation of functional synaptic connections between cultured cortical neurons from agrin-deficient mice. J. Neurobiol. 39, 547–557.
Longair, M.H., Baker, D.A., Armstrong, J.D., 2011. Simple neurite tracer: open source software for reconstruction, visualization and analysis of neuronal processes. Bioinformatics 27, 2453–2454.
Mann, S., Kröger, S., 1996. Agrin is synthesized by retinal cells and colocalizes with gephyrin. Mol. Cell. Neurosci. 8, 1–13.
McCarthy, K.D., de Vellis, J., 1980. Preparation of separate astroglial and oligodendroglial cell cultures from rat cerebral tissue. J. Cell Biol. 85, 890–902.
McCroskery, S., Bailey, A., Lin, L., Daniels, M.P., 2009. Transmembrane agrin regulates dendritic filopodia and synapse formation in mature hippocampal neuron cultures. Neuroscience 163, 168–179.
McMahan, U.J., 1990. The agrin hypothesis. Cold Spring Harb. Symp. Quant. Biol. 55, 407–418.
Neumann, F.R., Bittcher, G., Annies, M., Schumacher, B., Kröger, S., Ruegg, M.A., 2001. An alternative amino-terminus expressed in the central nervous system converts agrin to a type II transmembrane protein. Mol. Cell. Neurosci. 17, 208–225.
O'Connor, L.T., Lauterborn, J.C., Smith, M.A., Gall, C.M., 1995. Expression of agrin mRNA is altered following seizures in adult rat brain. Mol. Brain Res. 33, 277–287.
Pohlkamp, T., Durakoglugil, M., Lane-Donovan, C., Xian, X., Johnson, E.B., Hammer, R.E., Herz, J., 2015. Lrp4 domains differentially regulate limb/brain development and synaptic plasticity. PLoS One 10, e0116701.
Porten, E., Seliger, B, Schneider, V.A., Wöll, S., Stangel, D., Ramseger, R., Kröger, S., 2010. The process-inducing activity of transmembrane agrin requires follistatin-like domains. J. Biol. Chem. 285, 3114–3125.
Pribiag, H., Peng, H., Shah, W.A., Stellwagen, D., Carbonetto, S., 2014. Dystroglycan mediates homeostatic synaptic plasticity at GABAergic synapses. Proc. Natl. Acad. Sci. USA 111, 6810–6815.
Ramseger, R., White, R., Kröger, S., 2009. Transmembrane form agrin-induced process formation requires lipid rafts and the activation of Fyn and MAPK. J. Biol. Chem. 284, 7697–7705.
Rost, B.R., Breustedt, J., Schoenherr, A., Grosse, G., Ahnert-Hilger, G., Schmitz, D., 2010. Autaptic cultures of single hippocampal granule cells of mice and rats. Eur. J. Neurosci. 32, 939–947.
Schröder, J.E., Tegeler, M.R., Grosshans, U., Porten, E., Blank, M., Lee, J., Esapa, C., Blake, D.J., Kröger, S., 2007. Dystroglycan regulates structure, proliferation and differentiation of neuroepithelial cells in the developing vertebrate CNS. Dev. Biol. 307, 62–78.
Serpinskaya, A.S., Feng, G.P., Sanes, J.R., Craig, A.M., 1999. Synapse formation by hippocampal neurons from agrin-deficient mice. Dev. Biol. 205, 65–78.
Sun, X.D., Li, L., Liu, F., Huang, Z.H., Bean, J.C., Jiao, H.F., Barik, A., Kim, S.M., Wu, H., Shen, C., Tian, Y., Lin, T.W., Bates, R., Sathyamurthy, A., Chen, Y.J., Yin, D.M., Xiong, L., Lin, H.P., Hu, J.X., Li, B.M., Gao, T.M., Xiong, W.C., Mei, L., 2016. Lrp4 in astrocytes modulates glutamatergic transmission. Nat. Neurosci. 19, 1010–1018.
Swartz, M., Eberhart, J., Mastick, G.S., Krull, C.E., 2001. Sparking new frontiers: using in vivo electroporation for genetic manipulations. Dev. Biol. 233, 13–21.
Tian, Q.B., Suzuki, T., Yamauchi, T., Sakagami, H., Yoshimura, Y., Miyazawa, S., Nakayama, K., Saitoh, F., Zhang, J.P., Lu, Y., Kondo, H., Endo, S., 2006. Interaction of LDL receptor-related protein 4 (LRP4) with postsynaptic scaffold proteins via its C-terminal PDZ domain-binding motif, and its regulation by Ca/calmodulin-dependent protein kinase II. Eur. J. Neurosci. 23, 2864–2876.
Tintignac, L.A., Brenner, H.R., Ruegg, M.A., 2015. Mechanisms regulating neuromuscular junction development and function and causes of muscle wasting. Physiol. Rev. 95, 809–852.
Weatherbee, S.D., Anderson, K.V., Niswander, L.A., 2006. LDL-receptor-related protein 4 is crucial for formation of the neuromuscular junction. Development 133, 4993–5000.
Ye, X.C., Hu, J.X., Li, L., Li, Q., Tang, F.L., Lin, S., Sun, D., Sun, X.D., Cui, G.Y., Mei, L., Xiong, W.C., 2018. Astrocytic Lrp4 (low-density lipoprotein receptor-related protein 4) contributes to ischemia-induced brain injury by regulating ATP release and adenosine-A2AR (adenosine A2A receptor) signaling. Stroke 49, 165–174.
Zhang, B., Luo, S., Wang, Q., Suzuki, T., Xiong, W.C., Mei, L., 2008. LRP4 serves as a coreceptor of agrin. Neuron 60, 285–297.
Zhang, Y., Lin, S., Karakatsani, A., Rüegg, M.A., Kröger, S., 2015. Differential regulation of AChR clustering in the polar and equatorial region of murine muscle spindles. Eur. J. Neurosci. 41, 69–78.
Zucker, R.S., Regehr, W.G., 2002. Short-term synaptic plasticity. Annu. Rev. Physiol. 64, 355–405.